Characterization and Thiophene Hydrodesulfurization Activity of NaX Zeolite Supported Molybdena Catalysts

Debasish DAS,*,# Maya DUTTAGUPTA, and Sunanda K. PALIT
Department of Chemistry, Indian Institute of Technology, Kharagpur 721302, India
(Received December 27, 1993)

A series of NaX zeolite supported molybdena catalysts containing 1—15 wt% MoO_3 has been prepared by impregnation method. They have been characterized by X-ray diffraction (XRD), infrared spectroscopy (IR), temperature-programmed reduction (TPR), scanning electron microscopy (SEM), surface area, pore volume, Mo dispersion, and Mo extraction measurements. Zeolite crystallinity was found to be affected greatly only at 15 wt% MoO_3 loading. XRD and SEM studies showed absence of any crystalline MoO_3 phase. However, presence of bulk MoO_3, particularly at higher loadings, was indicated by TPR and Mo extraction results. Tetrahedral surface molybdenum species are formed through strong interaction between molybdena and zeolite lattice through oxygen atoms. A direct relationship between Mo dispersion on the oxidic catalysts and their thiophene conversion activity was observed. In addition to Mo dispersion, acidity of the catalysts was also found to play an important role at high reaction temperature.

Molybdena containing catalysts are widely used in many industrially important reactions like oxidation, alkene metathesis, and hydrotreatment reactions.[1—3] The conventional supported molybdena catalysts are prepared by using a suitable carrier like alumina, silica, or silica-alumina. However, in recent years there is an increasing interest in the preparation of zeolite supported molybdena or nickel molybdena hydrotreatment catalysts. Zeolites, as support, are used either alone or in combination with an amorphous counterpart like alumina or silica-alumina in the modern hydrotreatment catalysts.[4,5] The acidic nature, high thermal stability, and increased resistance towards organic sulfur and nitrogen compounds of the zeolites are found to play important role in hydrotreating processes. Molybdenum containing zeolites have been prepared by various techniques viz., impregnation, aqueous ion exchange, vapor phase adsorption, solid–solid reaction, and direct incorporation into zeolite lattice during the synthesis step. Dai and Lunsford[6] introduced molybdenum ions into Y zeolite by solid–solid exchange method and characterized them by IR, EPR, XPS, and XRD analyses. Okamoto et al.[7] reported highly dispersed molybdenum sulfide catalysts prepared from $Mo(CO)_6$ encaged in KY and NaY zeolites by treatment with H_2S at 373 K. Cid et al.[8] prepared molybdena impregnated NaY zeolite catalysts by conventional impregnation method. Their results showed that the crystallinity of their samples decreased almost linearly with molybdena loading. They also observed a strong interaction between molybdenum species and the zeolite lattice. A comparative study of diethylsulfide hydrodesulfurization using Ni, Mo, and Ni–Mo containing Y and ZSM-5 zeolite was also reported by Davidova et al.[9,10] Structural stability and thiophene HDS activity of molybdena impregnated NaY and NH_4NaY zeolite catalysts were also examined by Agudo et al.[11]

Although Y and ZSM-5 zeolite supported molybdena catalysts are found to deactivate rapidly due to coking by oligomerization of butenes on the acidic sites[12,13] still most of the studies reported so far concentrated primarily on Y and ZSM-5 zeolite supported systems. No such work has been done on X zeolite supported molybdena catalysts. Unlike Y or ZSM-5 zeolite, X zeolite being weakly acidic in nature (due to its lower Si/Al ratio) is expected to be less susceptible to deactivation by coke deposition. Hence, it will be of particular interest to study the physical properties and catalytic behavior of molybdena catalysts supported on X zeolite.

In this paper we report characterization of NaX zeolite supported molybdena catalysts by various physicochemical techniques, viz. X-ray diffraction, infrared spectroscopy, temperature programmed reduction, surface area, pore volume, water content, Mo extraction, and Mo dispersion measurements. Catalytic hydrodesulfurization (HDS) activity was investigated using thiophene as a model sulfur compound. A preliminary account of the characterization of the catalysts was reported earlier.[14]

Experimental

Catalyst Preparation. A series of Mo/NaX zeolites with different molybdena loadings were prepared from NaX zeolite (Union Carbide 13X) by wet impregnation with aqueous solutions of ammonium heptamolybdate. The volume of solution used was just sufficient to completely wet the zeolite sample. The water was evaporated at 80 °C under vacuum in a rotary evaporator. The catalysts were dried in air at 120 °C overnight and finally calcined in air at 500 °C for 6 h. The catalyst will be referred to hereafter as Mo/NaX(y), where y indicates the amount of molybdena in wt%.

A physical mixture of 15 wt% molybdena and NaX zeolite was prepared by mixing both the components in acetone and stirring in an ultrasonic bath for 20 min. The solvent was removed by vacuum evaporation and the solid material was

#Present address: Solid State Laboratory, Department of Chemistry, Indian Institute of Technology, Bombay 400076, India, Fax: 091 22 5783480.

dried at 120 °C for 2 h.

Catalyst Characterization. The molybdenum content of the catalysts was very close to the nominal value as determined by atomic absorption spectrometry (Table 1). Powder XRD patterns were recorded by a Philips PW 1729 diffractometer using nickel filtered Cu $K\alpha$ radiation. Degree of crystallinity of the catalysts was estimated by comparing the intensity of the three major diffraction lines (3 3 1, 5 3 3, and 7 5 1) with those of the parent NaX zeolite. The multipoint BET surface area and pore volume of the catalysts were obtained by N_2 adsorption at −196 °C using Quantasorb sorption system. Infrared spectra in the 1400—400 cm^{-1} region were recorded in a Perkin–Elmer 883 spectrophotometer using KBr disc technique. Equal amounts of the catalysts were well mixed with KBr in 1 : 100 ratio. Amount of free Mo on the catalysts was determined by extracting bulk molybdena with dilute ammonia solution (2 wt%) and analyzing the Mo content of the filtrate by visible spectrophotometry. Water content of the catalysts was determined by measuring the weight loss upon heating upto 600 °C in a Shimadzu DT-40 thermal analyser. Surface acidity of the catalysts was determined by titration with butylamine in dry benzene. The extent of molybdenum dispersion on the catalysts was determined by 1-butene chemisorption at 100 °C in a flow apparatus. The amount of 1-butene adsorbed by the catalysts was determined from TCD signals. Details about the method are given elsewhere.[15] TPR experiments were carried out in a conventional apparatus equipped with water and oxygen traps. 40 mg samples were packed in a quartz cell and heated in Ar flow at 400 °C for 2 h and then cooled down to room temperature. The sample was then reduced in 10% H_2 in Ar flow by heating at the rate of 10 °C min^{-1} to 750 °C and consumption of H_2 was monitored by a catharometric detector.

Catalytic Experiments. Catalytic experiments for thiophene hydrodesulfurization was carried out in atmospheric pressure using a fixed-bed down flow reactor. About 1 g of the catalyst (particle size 0.18—0.30 mm) were presulfided in situ in 10% (v/v) H_2S in H_2 at 400 °C for 2 h. Thiophene (1.2×10^{-2} mol h^{-1}) diluted in cyclohexane was fed by a peristaltic pump to the vaporizer, where it was mixed with H_2 (flow rate=60 ml min^{-1}) and then passed through the catalyst bed. Reaction products were analysed by a gas chromatograph using a 2 m Carbowax 20M column.

Results and Discussion

X-Ray Diffraction. X-Ray powder diffraction patterns of the calcined Mo/NaX zeolites along with those of parent NaX zeolite and the physical mixture of 15 wt% MoO_3 and NaX zeolite are shown in Fig. 1. All molybdena impregnated catalysts showed XRD patterns exactly similar to that of the NaX zeolite. While continuous decrease in the relative intensities of the lines was observed with increase in MoO_3 loading no such decrease was noticed in case of the physical mixture. This shows that such decrease in peak intensities can not be solely due to dilution effect and therefore, loss of crystallinity must also have taken place during MoO_3 incorporation. Fierro et al.[16] also observed such loss in crystallinity in Mo/NaY zeolite. They proposed that this occurs during the calcination process when MoO_3 migrates from external zeolite surface into the zeolite cavities. This redistribution process involves vaporization of MoO_3 in presence of water vapor according to the following equilibrium.

Table 1. Composition and Physical Properties of the Catalysts

Catalyst	MoO_3	S_{BET}	V_p	Crystallinity
	wt%	$m^2\,g^{-1}$	$cm^3\,g^{-1}$	%
NaX	—	650	0.35	100
Mo/NaX(1)	0.95	600	0.31	95
Mo/NaX(3)	2.85	570	0.24	85
Mo/NaX(7)	7.10	530	0.21	79
Mo/NaX(10)	10.05	500	0.18	74
Mo/NaX(15)	14.85	380	0.08	41

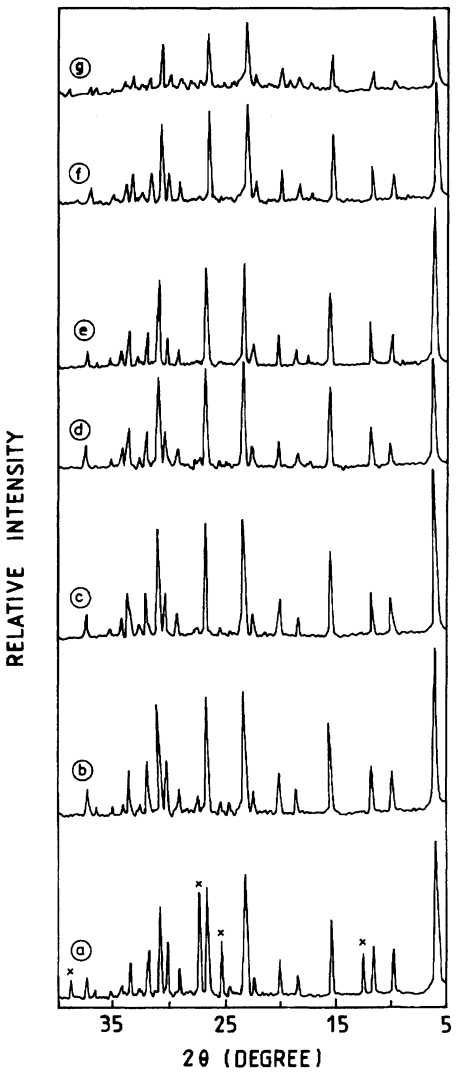

Fig. 1. X-Ray diffraction patterns of the catalysts: 15 wt% MoO_3+NaX physical mixture, (a); NaX, (b); Mo/NaX(1), (c); Mo/NaX(3), (d); Mo/NaX(7), (e); Mo/NaX(10), (f), and Mo/NaX(15), (g).

$$MoO_3 + H_2O(v) \rightleftharpoons MoO_2(OH)_2(v) \quad (1)$$

The $MoO_2(OH)_2$ then reacts with the zeolite surface oxygen atoms and becomes bonded to the zeolite lattice. We think that similar interaction between molybdate anions and zeolite lattice also occur in Mo/NaX zeolite which leads to the structure collapse and consequent loss in crystallinity in our samples. The average loss in crystallinity was calculated by comparing the peak intensities of the three major peaks (3 3 1, 5 3 3, and 7 5 1) with those for the parent NaX zeolite and is given in Table 1. Crystallinity was found to decrease almost linearly with increase in MoO_3 loading upto 10 wt% but was drastically reduced at 15 wt% loading.

No evidence for the presence of crystalline MoO_3 phase was found from the XRD patterns. The absence of crystalline MoO_3 phase implies that NaX zeolite supported molybdena primarily exists in an amorphous state or as small crystallites of less than 4 nm diameter. SEM studies also could not give any clear evidence for the presence of crystalline MoO_3 phase as only typical morphology of the zeolite crystals were observed.[15] It may be mentioned here that Cid et al.[8] also could not detect any crystalline MoO_3 phase in Mo/NaY zeolites. However, in case of the physical mixture we observed some XRD lines for MoO_3 phase (marked by cross in Fig. 1).

Surface Area and Pore Volume. The BET surface areas and pore volumes of the catalysts are presented in Table 1. The gradual decrease in surface area, which can be taken as measure of zeolite crystallinity, reflects that the crystalline structure of the zeolite was broken down or distorted by MoO_3 loading. This is possibly due to some kind of interaction between molybdate anions and the zeolite framework as also observed by Agudo et al.[11] in MoO_3/NaY zeolite. However, as zeolites have most of their surface area inside the cavities, blockage of pore openings by deposition of molybdate species would also result in reduction of surface area.

The pore volume of the catalysts were also showed a gradual decrease with increase in MoO_3 loading. Yong et al.[17] also observed similar decrease in pore volume of Mo/NaX catalysts prepared from $Mo(CO)_6$ and our results are also quite consistent with them. XPS analysis of Mo/NaY zeolites prepared by impregnation method showed that during calcination in presence of water vapor MoO_3 species migrate from the zeolite surface into the cavities.[16] From the absence of MoO_3 crystallites on the external surface as observed by XRD and SEM analyses it appears that MoO_3 species most probably remains inside the supercages of the zeolite. However, surface deposition of MoO_3 species can not be exclusively ruled out from these results.

Infrared Spectra. The mid-infrared spectra of the catalysts, parent NaX zeolite and the physical mixture are shown in Fig. 2. All MoO_3 loaded catalysts showed spectra of essentially similar in nature.

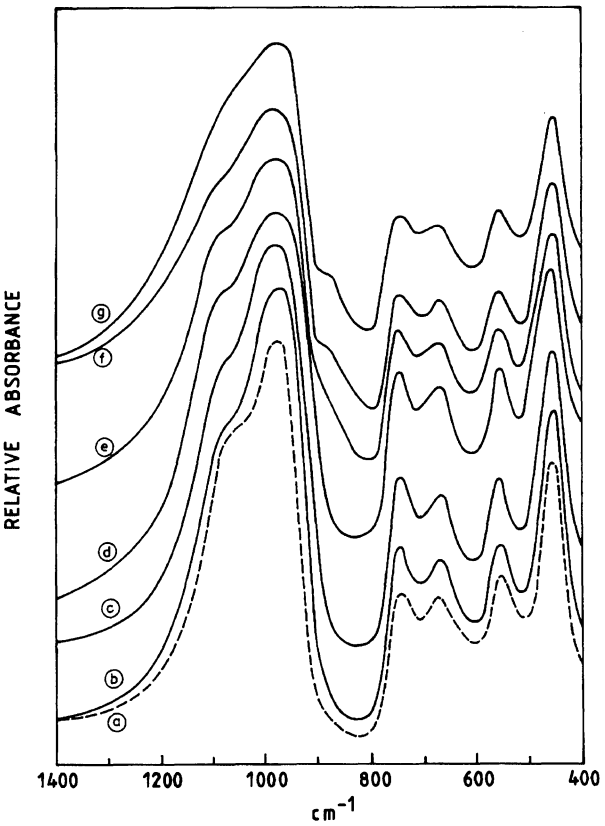

Fig. 2. Infrared spectra of the catalysts: 15 wt% MoO_3+NaX physical mixture, (a); NaX, (b); Mo/NaX(1), (c); Mo/NaX(3), (d); Mo/NaX(7), (e); Mo/NaX(10), (f), and Mo/NaX(15), (g).

Bands of varying intensity and width were observed at 1100, 975, 750, 675, 560, and 460 cm^{-1} which are typical of the parent NaX zeolite. The bands at 975 and 460 cm^{-1} are due to structure insensitive internal vibrations of the TO_4 (T=Si or Al) tetrahedra of NaX zeolite, whereas the other bands at 1100, 750, and 560 cm^{-1} are due to vibrations related to external linkages between the tetrahedra and are sensitive to structural change.[18] While intensity of the structure sensitive bands decreased significantly with increase in MoO_3 loading the structure insensitive bands did not show any significant change in position or intensity. The observed decrease in intensity of the structure sensitive bands indicate that there is increasing perturbation of the zeolite framework when MoO_3 loading is increased. This is in good agreement with the surface area and XRD results which showed interaction between zeolite lattice and MoO_3. Similar perturbation of zeolite lattice was also shown by infrared studies for thermally degraded NaY zeolites[18] and also for MoHY zeolites prepared by cation exchange.[6]

Although the position of the bands did not change with increasing molybdena loading a weak shoulder appeared at about 885 cm^{-1} at higher loading. It is reported that Mo–O bond vibrations give infrared active bands in the region 800—1000 cm^{-1}.[19] Absence of this

band in the physical mixture of MoO_3 and NaX zeolite, despite the presence of XRD lines, therefore, indicates that this band is not due to the MoO_3 phase but possibly due to some surface Mo–O band vibrations arising out of the interaction between molybdate anions and the surface hydroxyl groups of the zeolite lattice. Similar surface Mo–O band in the 890—900 cm^{-1} region was also observed in MoHY, Mo/NaY, and Mo/USY zeolites.[6,8,20] Earlier studies have indicated that the exact frequency of the Mo=O bond vibration depends on the coordination number and the number of terminal oxygen atoms on the molybdenum.[21] Recently Anderson et al.[20] has proposed the formation of tetrahedral surface molybdena species (**I**),

$$MoO_2(OH)_2 + 2\,(OH)_z \longrightarrow \underset{\text{(I)}}{\overset{O \quad O}{\diagdown\!\!\diagup \quad \diagdown\!\!\diagup}\;Mo\;\underset{O_z \quad O_z}{\diagdown\!\!\diagup \quad \diagdown\!\!\diagup}} + 2\,H_2O \qquad (2)$$

where z indicates oxygen atoms of zeolite lattice, in a similar manner as proposed for Al_2O_3.[22,23] The diffuse reflectance spectra of our Mo/NaX zeolites showed the presence of molybdenum in tetrahedral coordination with small amounts of octahedral molybdenum[14] and thereby indicates formation of such tetrahedral molybdena species on the Mo/NaX zeolite surface.

Water Content. The zeolite water content of the catalysts decreased continuously with increase in MoO_3 loading (Table 2). It is well known that in zeolites the water molecules sit inside the cavities/cages and therefore, the continuous decrease in water content suggests that the MoO_3 species must have replaced the water molecules and entered into the zeolite cavities. In Mo/NaY zeolite MoO_3 is reported to migrate from the external surface to the zeolite cavities during calcination.[16] Therefore, the observed decrease in water content is probably due to similar migration of MoO_3 species into the zeolite cavities.

Molybdenum Extraction. Since bulk MoO_3 readily dissolves in ammonia solution,[24] the fraction of Mo strongly attached to the zeolite framework was determined by treating the catalysts with dilute ammonia solution. It was shown that in medium-pore Mo/ZSM-5 zeolite most of the molybdena is deposited on the outer surface of the zeolite lattice and can be completely extracted with dilute ammonia.[13] Table 2 shows that a large fraction (>55%) of Mo was remained insoluble in our samples. This may be due to the reason that the fraction of molybdena retained inside the zeolite pores through attachment to the zeolite framework oxygen atoms are strongly held and are, therefore, difficult to extract. However, as MoO_3 loading was increased, larger fraction of it gets deposited at external zeolite surface and can be readily dissolved out with ammonia.

Comparison with an alumina supported molybdena catalyst (MoO_3=10 wt%) showed that in the alumina supported catalyst about 83% of Mo species can be extracted[15] which is almost twice the amount for zeolite supported catalyst with similar loading. This difference in extracted Mo between alumina and zeolite supported MoO_3 catalysts indicates that the interaction of molybdena with zeolite lattice is much stronger than that with alumina.

Surface Acidity. The total acidity of the catalyst is expressed in units of milliequivalent of amine added per m^2 of the catalyst to account for the catalyst surface area and are given in Table 2. A small decrease in total acidity of the NaX zeolite was observed with initial molybdena loading. However, with further increase in MoO_3 loading the acidity increased continuously.

Molybdenum Dispersion. The amount of 1-butene irreversibly adsorbed by the oxidic catalysts are given in Table 2. The values in units of mmol m^{-2} account for the catalyst surface area. The HDS activity of molybdena catalyst are known to be influenced by Mo dispersion in the catalysts.[25,26] Mo dispersion was found to increase with increasing MoO_3 loading, as indicated by continuous increase in 1-butene adsorption and also reflected by the thiophene conversion results (see below). However, at 15 wt% MoO_3 loading there was a decrease in Mo dispersion. This is not quite unexpected as similar decrease in Mo dispersion was also noticed in alumina supported molybdena catalysts at high MoO_3 loading.[27] Although we could not measure Mo dispersion on the sulfided catalysts we assume that the trend is same on the sulfided samples also. This is supported by Anderson et al.[28] who observed similar behavior on Mo–USY zeolites. They found by NO chemisorption that while samples prepared from $Mo(CO)_6$ and $MoCl_5$ show an increase in the number of

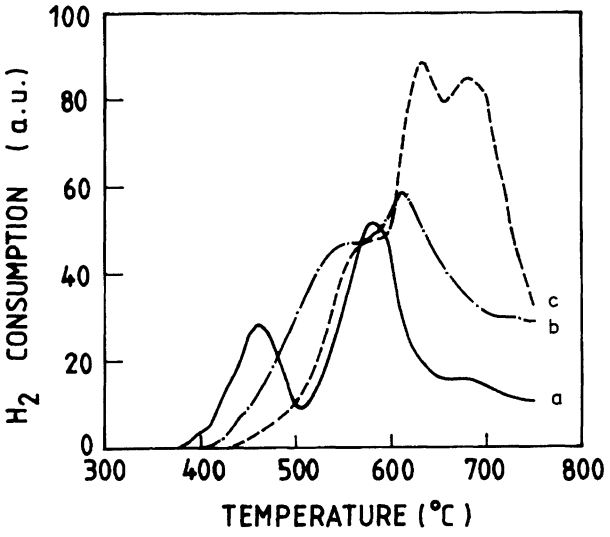

Fig. 3. Temperature programmed reduction spectra of the catalysts: Mo/NaX(7), (a); Mo/NaX(10), (b), and Mo/NaX(15), (c).

Table 2. Free Molybdenum, Water Content, Total Acidity, and Dispersion of Molybdenum on the Catalysts

Catalyst	Extracted Mo	Water content[a)]	Total acidity	Amount of 1-butene adsorbed
	%	%	(mequiv m^{-2}) $\times 10^{-4}$	(μmol m^{-2}) $\times 10^{-3}$
NaX	—	23.3	7.4	—
Mo/NaX(1)	22	23.2	7.0	1.5
Mo/NaX(3)	26	22.0	8.1	2.5
Mo/NaX(7)	30	21.2	8.9	5.3
Mo/NaX(10)	35	19.2	9.8	6.4
Mo/NaX(15)	44	13.0	14.5	5.3

a) Weight loss upto 600 °C.

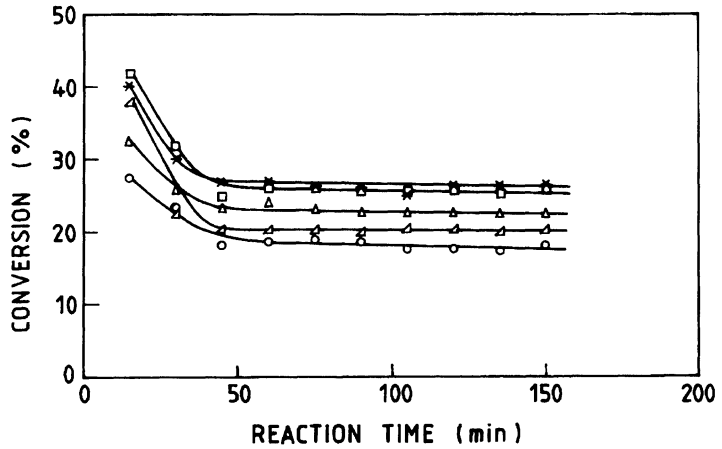

Fig. 4. Thiophene conversion at 350 °C vs. reaction time: Mo/NaX(1), (○); Mo/NaX(3), (△); Mo/NaX(7), (×); Mo/NaX(10), (□), and Mo/NaX(15), (◿).

NO adsorption sites after sulfidation, those prepared with ammonium heptamolybdate impregnation display an equivalent number of such sites.

Temperature-Programmed Reduction (TPR). The TPR spectra of the Mo/NaX(7), Mo/NaX(10), and Mo/NaX(15) catalysts are shown in Fig. 3. The initial temperature of reduction was found to increase with increasing MoO_3 loading. Thus, reduction starts at 375 °C in Mo/NaX(7) catalyst while it shifts to 420 °C in the Mo/NaX(15) catalyst. Since bulk crystals of MoO_3 reported to have some induction period in reduction[8,29)] this shift towards higher temperature might be due to the presence of such species at higher MoO_3 loading. Mo extraction results indeed showed the presence of bulk or free MoO_3 species in the catalysts at higher loadings. The TPR spectra also clearly show that reduction of the samples containing lower MoO_3 loading was complete at much lower temperature than those containing high MoO_3 loading.

Figure 3 shows that the shape of the TPR spectra of the catalysts are quite different in the three cases. In Mo/NaX(7) sample the characteristic two-peaks pattern of MoO_3 has been observed while these peaks started merging in the other two catalysts. The first peak has been attributed to Mo multilayers[30)] which appears to be quite reasonable as the size of this peak increased with increase in MoO_3 loading. As bulk MoO_3 shows two peaks at about 735 and 860 °C, shifting of the peak maxima position towards higher temperature at higher loadings indicates presence of bulk MoO_3 in the catalysts.

Catalytic Activity. Typical results of thiophene hydrodesulfurization vs. time-on-stream for the catalysts are shown in Fig. 4. Catalytic activity was high at the initial level but decreased with time-on-stream, presumably due to coking. It was observed that although the activity of the catalysts decreased initially they attained stable catalytic activity after about 60 min of reaction time. The initial drop in activity was found to increase with increasing MoO_3 loading, which is due to the rise in acidity of the catalysts (Table 2) and thereby resulting in more coke formation on the catalysts. In fact when the activity at initial and stable level are compared it was found that this drop in activity is directly related to the acidity of the catalysts.

Figure 4 also shows that the initial thiophene HDS activity of the catalysts increases with increase in molybdenum dispersion on the oxidic catalysts. High activity was shown by the Mo/NaX(10) catalyst which also showed highest molybdenum dispersion. Thus,

Table 3. Pseudo-First Order Rate Constant of the Catalysts

Catalyst	$k_{HDS} \times 10^{-3}$(mol h^{-1} g^{-1})		
	300 °C	350 °C	400 °C
Mo/NaX(1)	1.67	2.31	2.53
Mo/NaX(3)	2.38	3.06	3.14
Mo/NaX(7)	2.67	3.61	3.45
Mo/NaX(10)	2.90	3.53	2.83
Mo/NaX(15)	2.53	2.68	2.24

there is a direct relationship between initial conversion and molybdenum dispersion on the oxidic catalysts, although the relationship is not linear after the catalysts attained stable activity. This suggests that molybdenum dispersion on the sulfided catalysts has the same trend as on the oxidic catalysts. It may be mentioned here that similar observation was also reported by Anderson et al.[28] for Mo–USY zeolites. At stable activity, the catalyst with 7 and 10 wt% MoO_3 loadings have shown very similar conversion. That catalytic activity does not change in proportion to the molybdenum dispersion may be related to the difference in the rate of deactivation of these two catalysts. The crossover in activity of Mo/NaX(7) and Mo/NaX-(10) catalysts is thus due to higher acidity of the latter.

The pseudo-first order rate constant of the catalysts at 120 min are presented in Table 3. The activity of the catalysts was found to increase with rise in reaction temperature from 300 to 350 °C. Good correlation between molybdenum dispersion and catalytic activity was observed at 300 °C but at higher temperature this trend changes. Thus, while at 300 °C Mo/NaX-(10) showed higher activity than Mo/NaX(7), at 350 °C this trend was reversed. This is because the deactivation rate of Mo/NaX(10) at 350 °C is higher than that for Mo/NaX(7) due to higher acidity of Mo/NaX-(10). Further increase in reaction temperature results in decrease in activity in most of the catalysts except those with lower MoO_3 loading. This again suggests that at higher temperature acidity of catalysts plays an important role than molybdenum dispersion on the catalysts.

Conclusions

NaX zeolites supported molybdena catalysts prepared by impregnation technique suffer from large crystallinity loss only at high MoO_3 loading. MoO_3 is found to be present mostly in an amorphous state in the samples. While TPR and Mo extraction results indicate presence of bulk MoO_3 phase, particularly at higher loadings, no clear evidence for the presence of crystalline MoO_3 phase was found from XRD and SEM studies. Tetrahedral surface molybdenum species are formed through strong interaction between molybdena and zeolite lattice through oxygen atoms. At lower loadings MoO_3 species mostly remain inside the zeolite cages while at higher loadings it gets deposited on the external zeolite surface. Thiophene conversion activity of the catalysts are related to Mo dispersion and acidity of the catalysts.

References

1) J. Haber, "Proceedings of 3rd International Conference on the Chemistry and Uses of Molybdenum," ed by H. F. Barry and P. C. H. Mitchell, Climax Molybdenum Co., Ann Arbor, MI (1979), p. 114.
2) F. E. Massoth, *Adv. Catal.*, **26**, 265 (1979).
3) P. Ratnasamy and S. Sivasanker, *Catal. Rev. Sci. Eng.*, **22**, 401 (1980).
4) E. T. Child and D. A. Messing, U. S. Patent 3567602 (1971).
5) J. T. Miller, U. S. Patent 4812224 (1989).
6) P. S. E. Dai and J. H. Lunsford, *J. Catal.*, **64**, 173 (1980).
7) Y. Okamoto, A. Maezawa, H. Kane, and T. Imanaka, *J. Mol. Catal.*, **52**, 337 (1989).
8) R. Cid, F. J. Gil Llambias, J. L. G. Fierro, A. L. Agudo, and J. Villasenor, *J. Catal.*, **89**, 478 (1984).
9) N. Davidova, P. Kovacheva, and D. Shopov, *Stud. Surf. Sci. Catal.*, **24**, 659 (1985).
10) N. Davidova, P. Kovacheva, and P. Shopov, *Stud. Surf. Sci. Catal.*, **28**, 811 (1986).
11) A. L. Agudo, R. Cid, F. Orellana, and J. L. G. Fierro, *Polyhedron*, **5**, 187 (1986).
12) M. Laniecki and W. Zmierczak, *Zeolites*, **11**, 18 (1991).
13) A. L. Agudo, A. Benitez, J. L. G. Fierro, J. M. Palacios, J. Neira, and R. Cid, *J. Chem. Soc., Faraday Trans.*, **88**, 385 (1992).
14) D. Das, M. Duttagupta, and S. K. Palit, *J. Mater. Sci. Lett.*, **11**, 1078 (1992).
15) D. Das, Ph. D Thesis, Indian Institute of Technology, Kharagpur, India, 1992.
16) J. L. G. Fierro, J. C. Conesa, and A. L. Agudo, *J. Catal.*, **108**, 334 (1987).
17) Y. S. Yong and R. F. Howe, *Stud. Surf. Sci. Catal.*, **28**, 883 (1986).
18) E. M. Flanigen, H. Khatami, and H. A. Szymanski, *Adv. Chem. Ser.*, **101**, 201 (1971).
19) P. Gallezot, G. Coudurier, M. Primet, and B. Imelik, *Am. Chem. Soc. Symp. Ser.*, **40**, 144 (1977).
20) J. A. Anderson, B. Pawelec, and J. L. G. Fierro, *Appl. Catal.*, **99**, 37 (1993).
21) P. C. H. Mitchell and F. Trifirò, *J. Chem. Soc. A*, **1970**, 3138.
22) E. Furimski, *Catal. Rev. Sci. Eng.*, **22**, 371 (1980).
23) Y. Okamoto, Y. Katoh, Y. Mori, T. Imanaka, and S. Teranishi, *J. Catal.*, **70**, 445 (1981).
24) N. Giordano, J. C. J. Bart, A. Vaghi, A. Castellan, and G. Martinotti, *J. Catal.*, **36**, 81 (1975).
25) M. Houalla, C. L. Kibby, L. Petrakis, and D. M. Hercules, *J. Catal.*, **83**, 50 (1983).
26) R. Badilla-Ohlbaum and D. Chadwick, *Stud. Surf. Sci. Catal.*, **7**, 1126 (1980).
27) J. L. G. Fierro, *Stud. Surf. Sci. Catal.*, **57B**, 55 (1990).

28) J. A. Anderson, B. Pawelec, and J. L. G. Fierro, *Appl. Catal.*, **99**, 55 (1993).
29) P. Gajardo, P. Grange, and B. Delmon, *J. Chem. Soc., Faraday Trans. 1*, **76**, 929 (1980).
30) R. Thomas, E. M. van Oers, V. H. J. de Beer, J. Medena, and J. A. Moulijn, *J. Catal.*, **76**, 241 (1982).